Supplementary Table 1. RT-qPCR primers

Primer name	Sequence	Amplified regions
CD133-F	TTGTGGCAAATCACCAGGTA	NM_006017.2
CD133-R	TCAGATCTGTGAACGCCTTG	742-903
KRT19-F	TTTGAGACGGAACAGGCTCT	NM_002276.4
KRT19-R	AATCCACCTCCACACTGACC	647-857
LAD1-F	ACCTACAGCAGCTCCCTCAA	NM_005558.3
LAD1-R	ATGGCCGTGTGGTATCTCTC	1316-1479
SHE-F	AAGCAGCAAGAGACGGTCAT	NM_001010846.2
SHE-R	TCACAGGGACTGTCAAGCAG	601-809
ID1-F	AAACGTGCTGCTCTACGACA	NM_181353.2
ID1-R	TAGTCGATGACGTGCTGGAG	291-407
GAPDH-F	CGACCACTTTGTCAAGCTCA	NM_001289746.1
GAPDH-R	AGGGGAGATTCAGTGTGGTG	1086-1288

Supplementary Table 2. Sequenom MassARRAY primers

Primer name	Sequence	Amplified regions
CD133-F	GTTAGATGGAGAATTGGGGTGTTTA	NC_000004.11, Chr4: 16084085-16084583
CD133-R	AACTCCAAAAACAACCTATTACAAAA	
KRT19-F	TATTTTGTTTAGGTAGGAGGTTAGG	NC_000017.10, Chr17: 39684206-39684672
KRT19-R	CTCTCAAAAACCTACAAATTCCTCA	
LAD1-F	TTTAAAGTTTAGTATTAGGGAGTAAGGA	NC_000001.10, Chr1: 201368747-201369194
LAD1-R	AAAACTTCCTACTCAAAACCAATCC	
SHE-F	AAGTGGTTTAAGGAGTTTTTTTTGAA	NC_000001.10, Chr1: 154473923-154474385
SHE-R	ACTTAATAATCTTACCCTTATCCAACTC	
ID1-F	TTAGGGATTTTTAGTTGGAGTTGAA	NC_000020.10, Chr20: 30193495-30193949
ID1-R	TTCCTCTTACCCCCTAAATAACTAAA	

Supplementary Table 3. (h) MeDIP-qPCR and ChIP-qPCR primers

Primer name	Sequence	Amplified regions
CD133-F	CCCAGTGGATGGAAAGAAGA	NC_000004.11, Chr4:16084979-16085207
CD133-R	ACTGGGGGTGTACAGTGAGG	
KRT19-F	GTCGCGGATCTTCACCTCTA	NC_000017.10, Chr17:39684158-39684346
KRT19-R	TTTGTGTCCTCGTCCTCCTC	
LAD1-F	TAGGCCTCGCTGAGATGAAT	NC_000001.10, Chr1:201369024-201369172
LAD1-R	CAAGGACAGTGCCTTTGACA	
SHE-F	GTCCACCTTGATGAGCCTGT	NC_000001.10, Chr1:154474050-154474184
SHE-R	AGCCTGCAGGGTCTGATTC	
ID1-F	AAACGTGCTGCTCTACGACA	NC_000020.10, Chr20:30193376-30193492
ID1-R	TAGTCGATGACGTGCTGGAG	
C1orf14-F	CAGCACTTCGTCGCAATACA	NC_000001.10, Chr1:182921876-182921983
C1orf14-R	GTGCCTGAGGATGAAGAGGA	
Evpl-1F	GGCTTTCTGCTGTTTCTGCT	NT_165773.2, Chr11:27624419-27624638
Evpl-1R	CCGAGTGTGGGAGATCCTTA	
H2-T22-F	CTCAGGGGACATGGAGTGAT	NT_039649.7, Chr17:22362837-22362982
H2-T22-R	AGTATTGGGAGCGGGAGACT	
Kcng1-F	GAGCTGCTGACGGTCTTACC	NT_039207.7, Chr2:109135252-109135352
Kcng1-R	CCTGTCCGTTCTGTTTGTCA	
Slc25a31-F	GCGTCCTCCAAGCAGATAAG	NT_039229.7, Chr3:58531-58646
Slc25a31-R	TATGGGATGCTAAGGCCAAG	
D1pas1-F	TGACAAAGCAGACGAGGATG	NT_039189.7, Chr1:3464325-3464463
D1pas1-R	GTTATTCCCTGTCGCCTCAA	
Actl7b-F	CTGGGCAGAGGAGACTCAAC	NT_109315.4, Chr4:14592202-14592309
Actl7b-R	CTGGCTTCAAGGAGGAGATG	

Supplementary Figure Legends

Supplementary Figure S1. Identification of 293T cells overexpressing TET2-WT and TET2-Mut. (A) Immunofluorescence analysis of TET2 in Mock, TET2-WT, and TET2-Mut 293T cells. (B) Immunofluorescence analysis of 5hmC in Mock, TET2-WT, and TET2-Mut 293T cells. (C) Dot blot analysis of 5hmC and 5mC in Mock, TET2-WT, and TET2-Mut 293T cells.

Supplementary Figure S2. Numbers of DHMRs (A) and DMRs (B) in TET2-WT and TET2-Mut cells (*vs.* Mock cells) at CGIs.

Supplementary Figure S3. MeDIP-qPCR analysis for 5mC at four representative hypermethylated CGIs. The *ID1* gene CGI was used as a negative control. Data are presented as mean ± SD (n=3). **P*<0.05.

Supplementary Figure S4. Effect of TET2 overexpression on H3K4me1, H3K4me2, H3K9me2 and H3K9me3 enrichment at four representative hypermethylated CGIs in 293T cells. ChIP-qPCR analysis of H3K4me1 (A), H3K4me2 (B), H3K9me2 (C), and H3K9me3 (D) in Mock, TET2-WT, and TET2-Mut 293T cells. The *ID1* gene CGI was used as a control. Data are presented as mean ± SD (n=3). **P*<0.05.

Supplementary Figure S5. ChIP-qPCR analysis of histone H3 occupation at four representative hypermethylated CGIs in Mock, TET2-WT, and TET2-Mut 293T cells. *ID1* and *C1orf14* gene CGIs were used as a control. Data are presented as mean ± SD (n=3). **P*<0.05.

Supplementary Figure S6. Effect of TET2 overexpression on the global levels of histone modifications in 293T cells. Representative Western blot analysis of the global H3K4me3 and H3K27me3 levels in Mock, TET2-WT, and TET2-Mut 293T cells. Histone H4 was used as loading control.

Supplementary Figure S7. RT-qPCR analysis of the mRNA expression of four representative hypermethylated CGI genes in Mock, TET2-WT, and TET2-Mut 293T cells. The *ID1* gene was used as a control. The mRNA expression levels are normalized to the value in Mock cells. Data are presented as mean ± SD (n=6). **P*<0.05.

Supplementary Figure S8. Effect of 5-Aza-CdR treatment on the bivalency formation at the representative CGI promoters and the gene expression of corresponding genes. (A) H3K4me3 ChIP-qPCR analysis. (B) H3K27me3 ChIP-qPCR analysis. (C) RT-qPCR analysis. (D) Sequential ChIP-qPCR analysis of 5-Aza-CdR-treated 293T cells. Upper panel is the result of the 1st ChIP using IgG and anti-H3K4me3 Ab. Lower panel is the result of the 2nd ChIP using IgG and anti-H3K27me3 Ab. The % IP in the 2nd ChIP was plotted relative to input in the eluate from the first round ChIP. *ID1* gene was used as a control for all data. All data are presented as mean ± SD (n=3). **P*<0.05.

Supplementary Figure S9. Venn diagram shows the overlapping of H3K4me3 peaks (A), H3K27me3 peaks (B) and bivalent domains (C) between Mock and TET2-WT 293T cells.

Supplementary Figure S10. UCSC browser snapshots of H3K4me3 and H3K27me3 enrichment on two representative hypermethylated CGI genes (*LAD1* and *SHE*).

Supplementary Figure S11. Venn diagram shows the overlapping of H3K4me3 peaks (A), H3K27me3 peaks (B) and bivalent domains (C) at CGIs between Mock and TET2-Mut 293T cells.

Supplementary Figure S12. (A) Gene ontology (GO) analysis of the "gain-of-bivalency" genes in TET2-WT 293T cells compared with Mock 293T cells. (B) Venn diagram shows the overlapping between the "gain-of-bivalency" genes in

TET2-WT 293T cells and the bivalent genes in human ES cells.

Supplementary Figure S13. Average distribution patterns of 5mC (A), 5hmC (B), H3K4me3 (C) and H3K27me3 (D) across 4010 reported bivalent domains in wild type (Black) and *Tet1/2*-DKO (Blue) mouse ES cells.

Supplementary Figure S14. MeDIP-qPCR, hMeDIP-qPCR, and ChIP-qPCR analysis of 5mC (A), 5hmC (B), H3K4me3 (C), and H3K27me3 (D) enrichment at several selected CGIs in wild type and *Tet1/2*-DKO mouse ES cells. Data are presented as mean ± SD (n=3). **P*<0.05.

Supplementary Figure S1

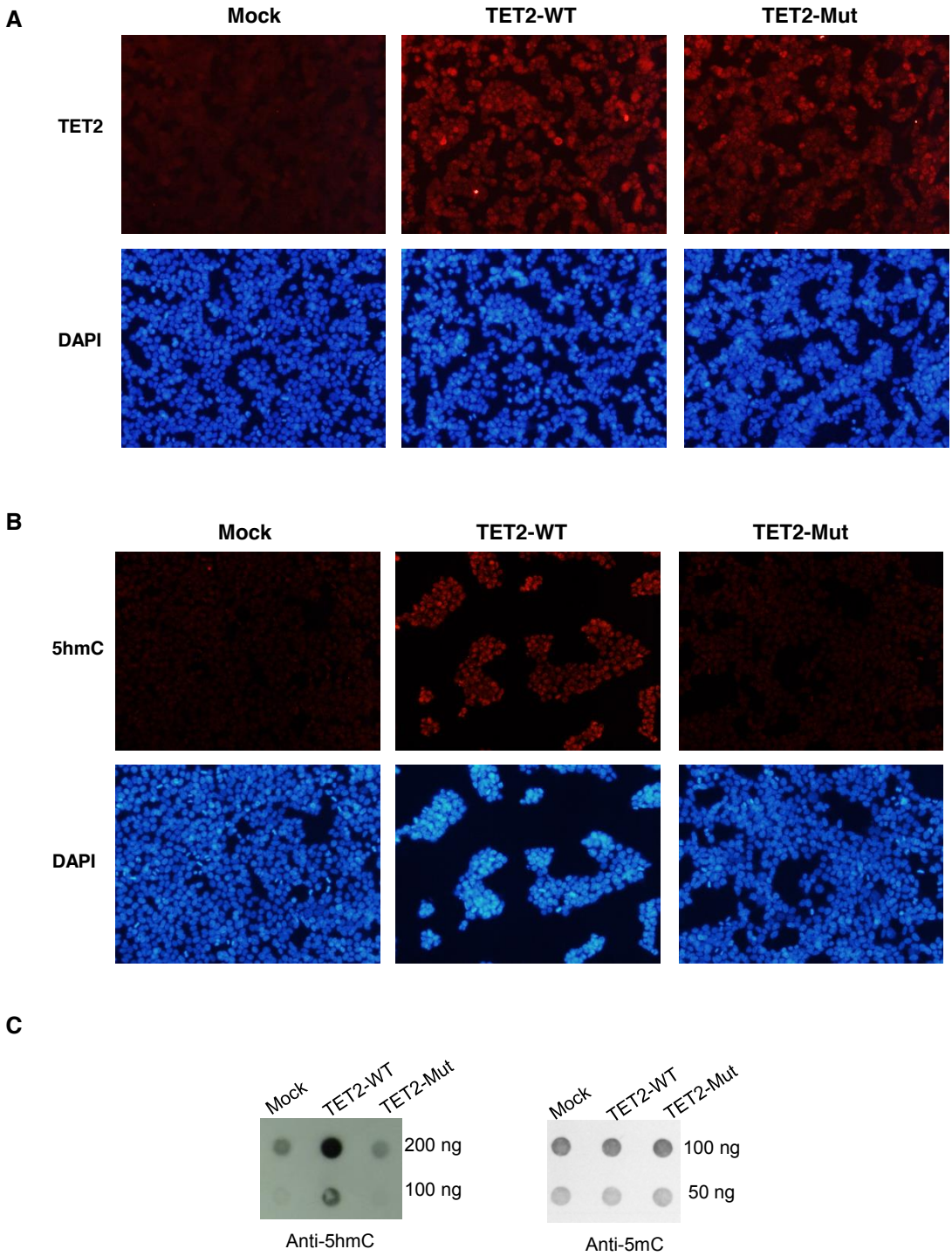

Supplementary Figure S2

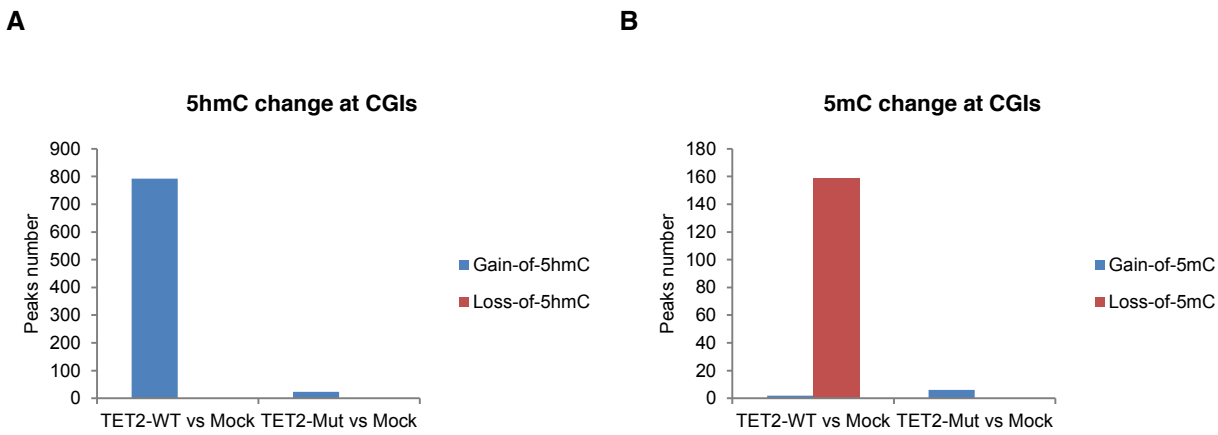

Supplementary Figure S3

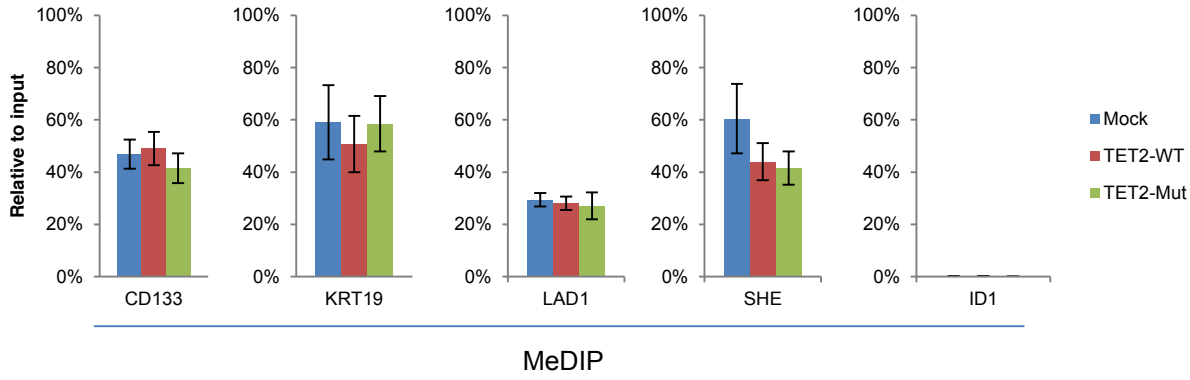

Supplementary Figure S4

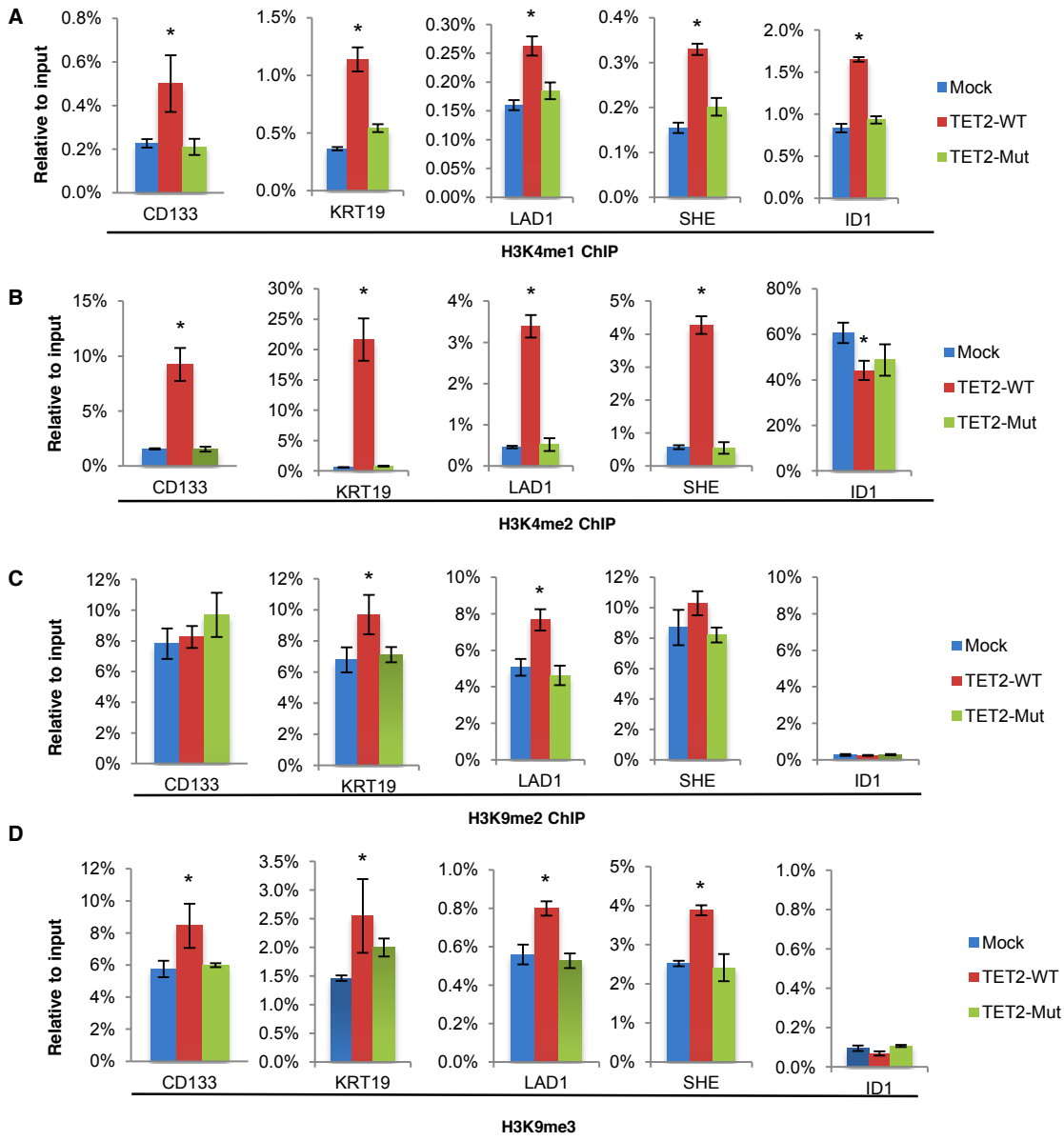

Supplementary Figure S5

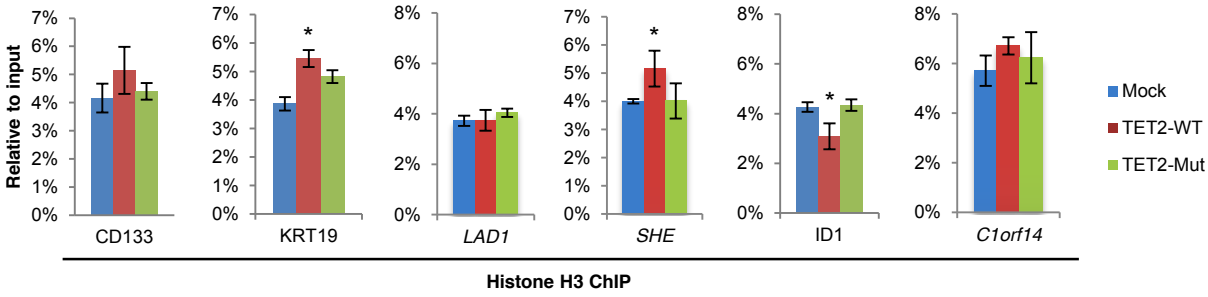

Supplementary Figure S6

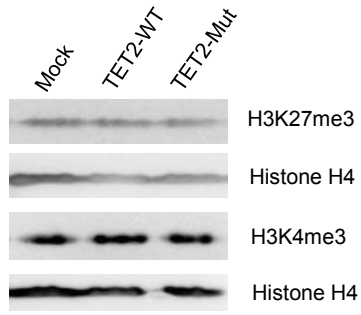

Supplementary Figure S7

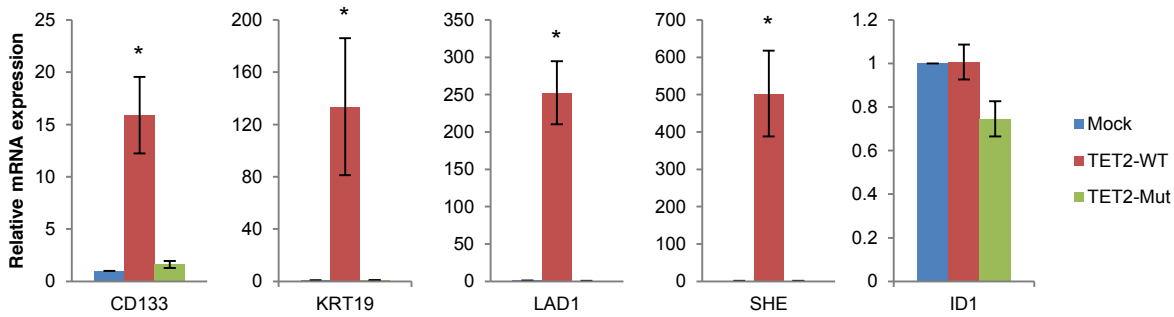

Supplementary Figure S8

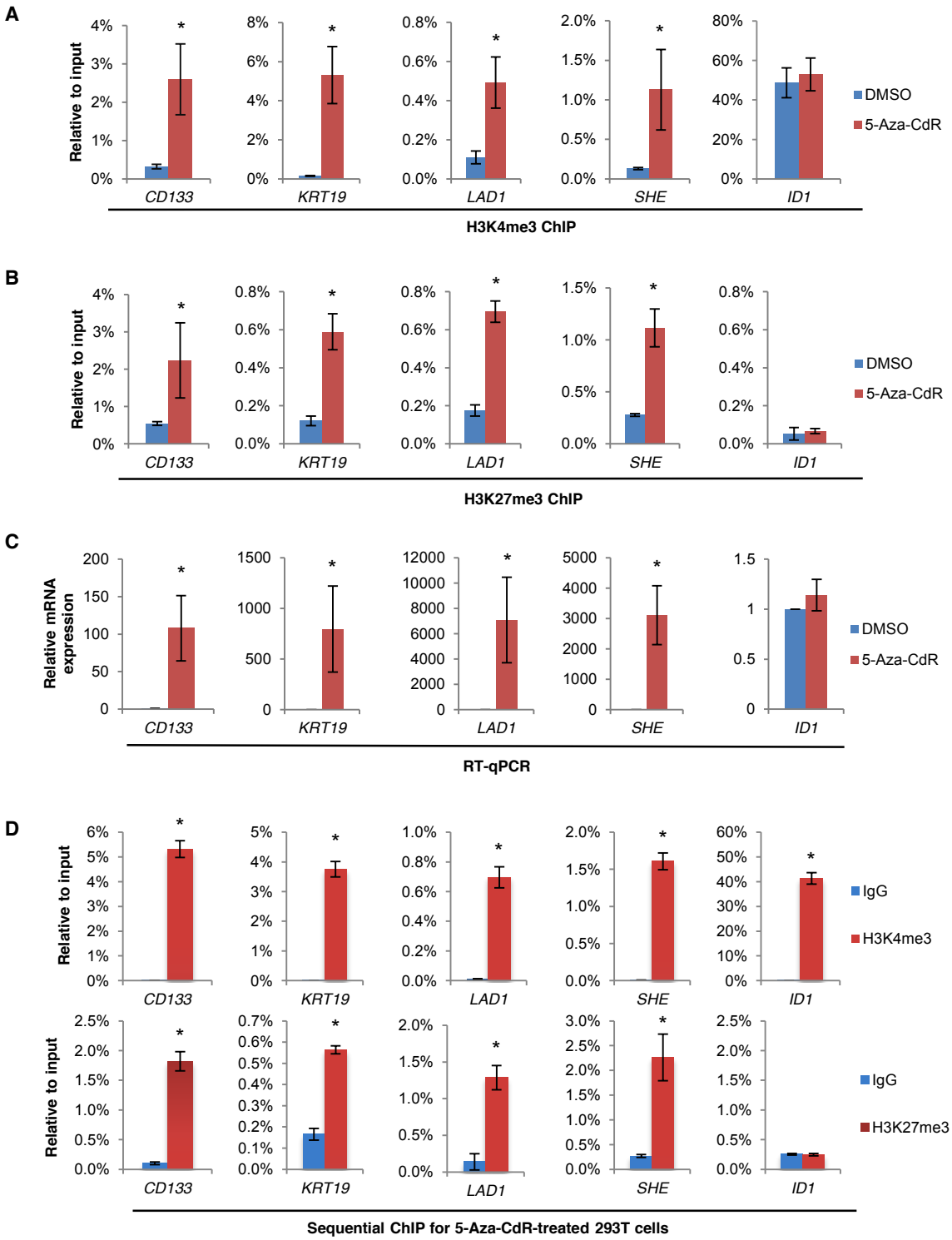

Supplementary Figure S9

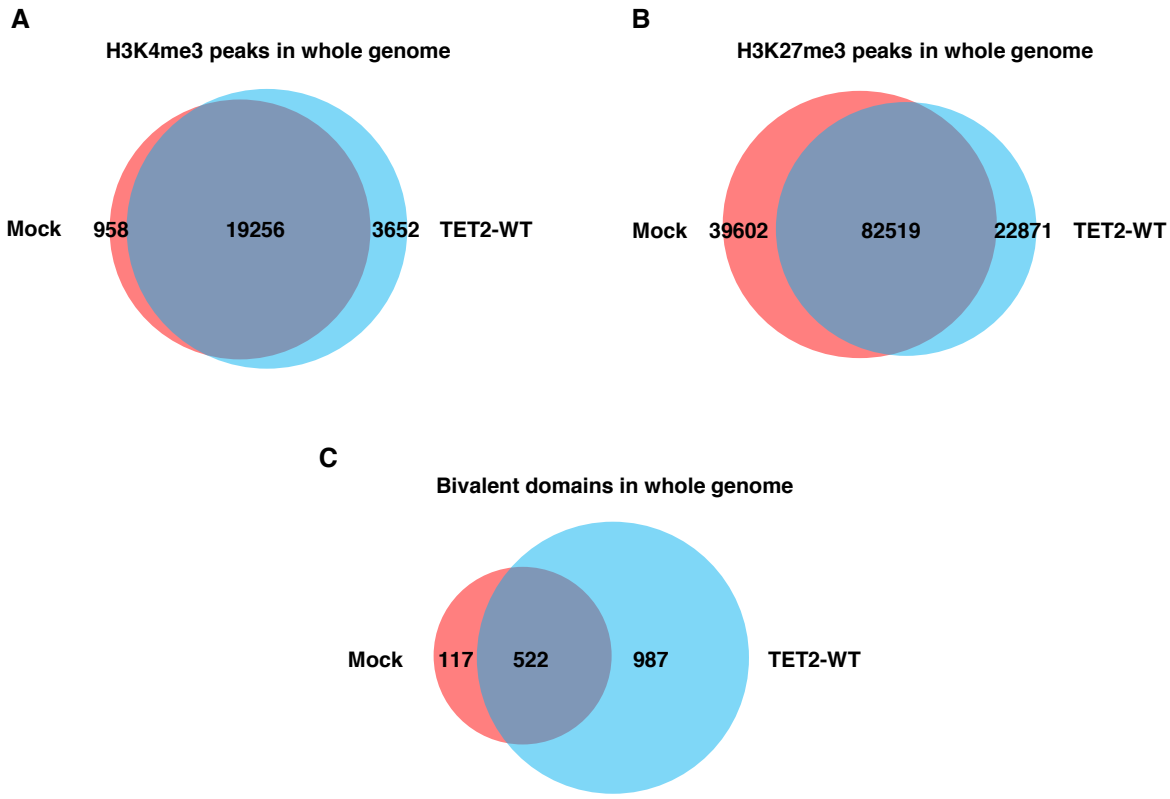

Supplementary Figure S10

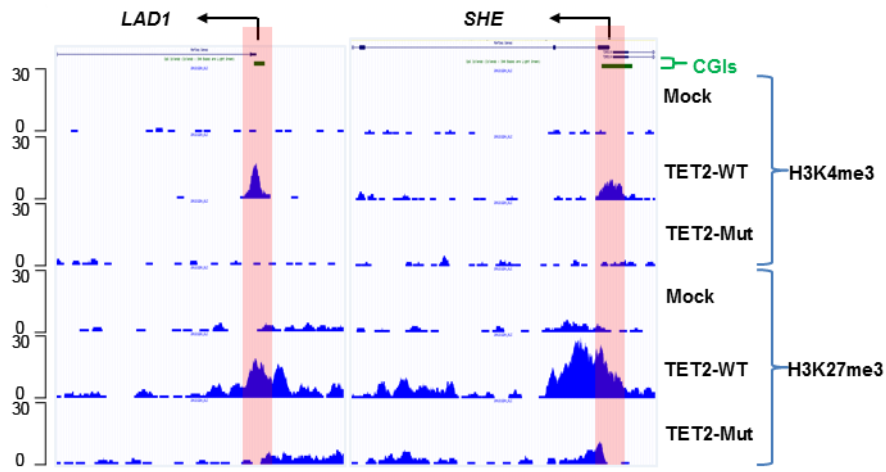

Supplementary Figure S11

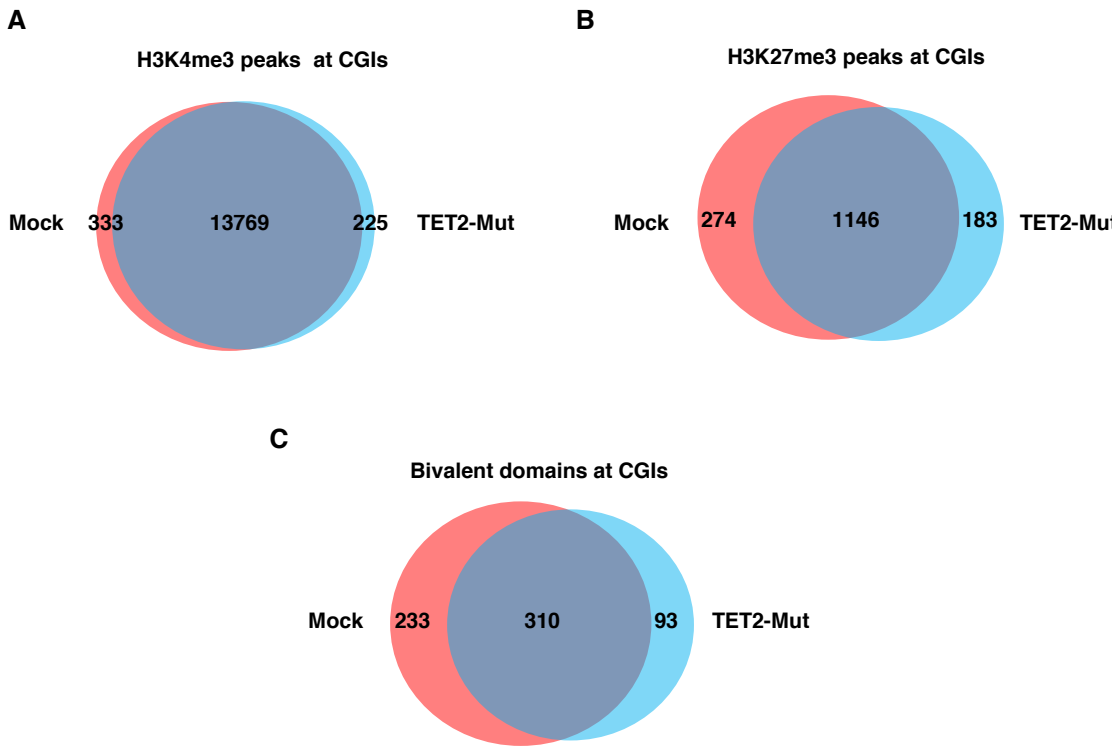

Supplementary Figure S12

A

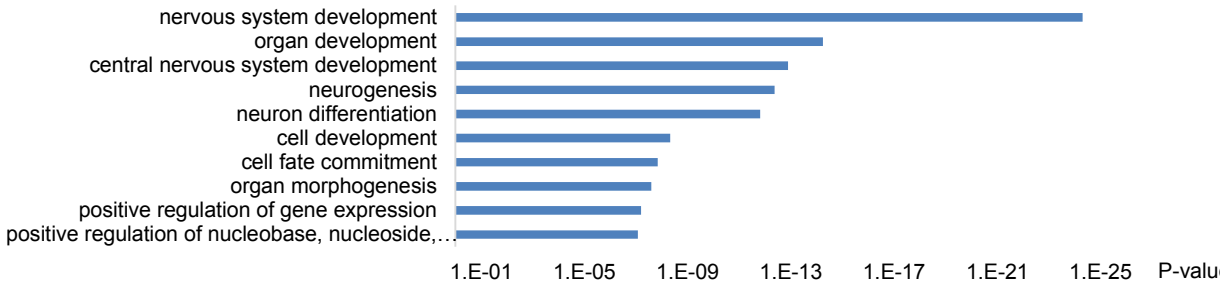

B

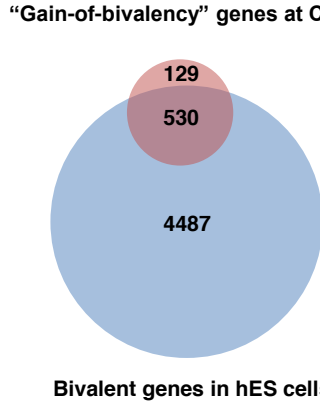

Supplementary Figure S13

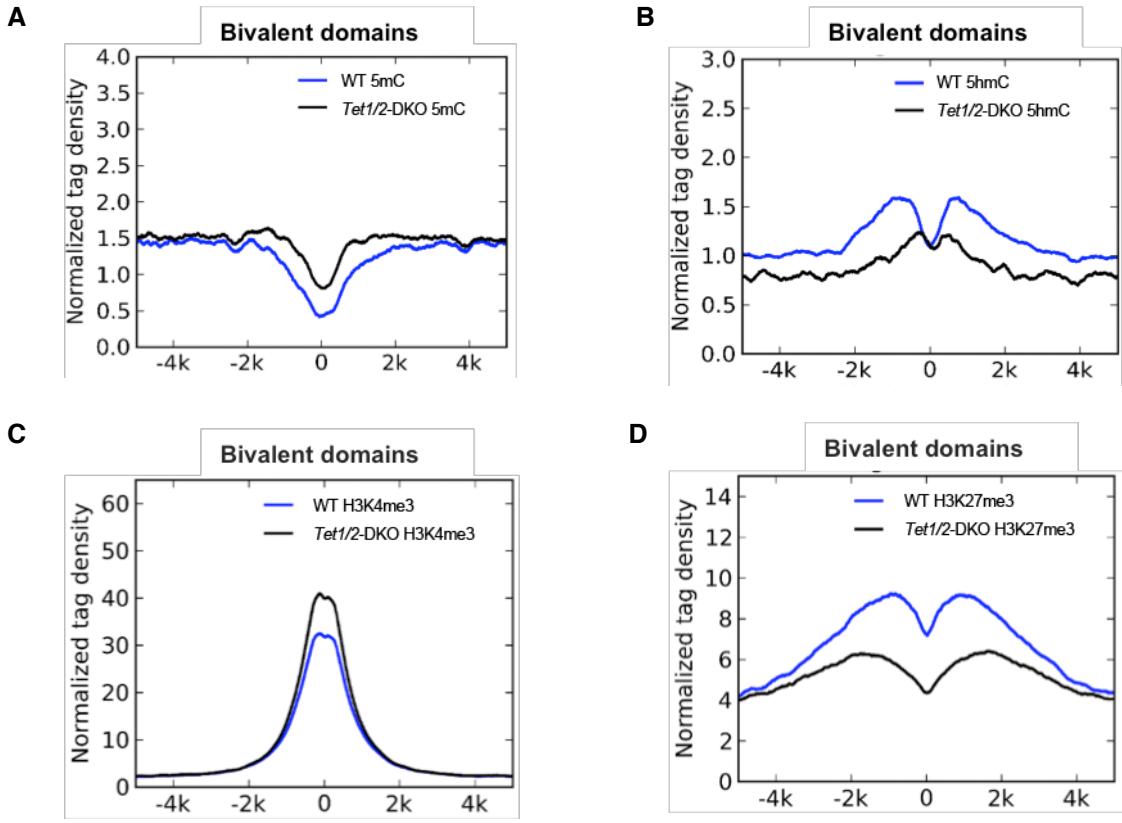

Supplementary Figure S14